2017

Pneumocystis-driven inducible bronchus-associated lymphoid tissue formation requires Th2 and Th17 immunity

Taylor Eddens
Children's Hospital of Pittsburgh at UPMC

Waleed Elsegeiny
Children's Hospital of Pittsburgh at UPMC

Maria de la Luz Garcia-Hernandez
University of Rochester

Patricia Castillo
Children's Hospital of Pittsburgh at UPMC

Giraldina Trevejo-Nunez
Children's Hospital of Pittsburgh at UPMC

See next page for additional authors

Authors
Taylor Eddens, Waleed Elsegeiny, Maria de la Luz Garcia-Hernandez, Patricia Castillo, Giraldina Trevejo-Nunez, Katelin Serody, Brian T. Campfield, Shabaana A. Khader, Kong Chen, Javier Rangel-Moreno, and Jay K. Kolls

Article

Cell Reports

Pneumocystis-Driven Inducible Bronchus-Associated Lymphoid Tissue Formation Requires Th2 and Th17 Immunity

Graphical Abstract

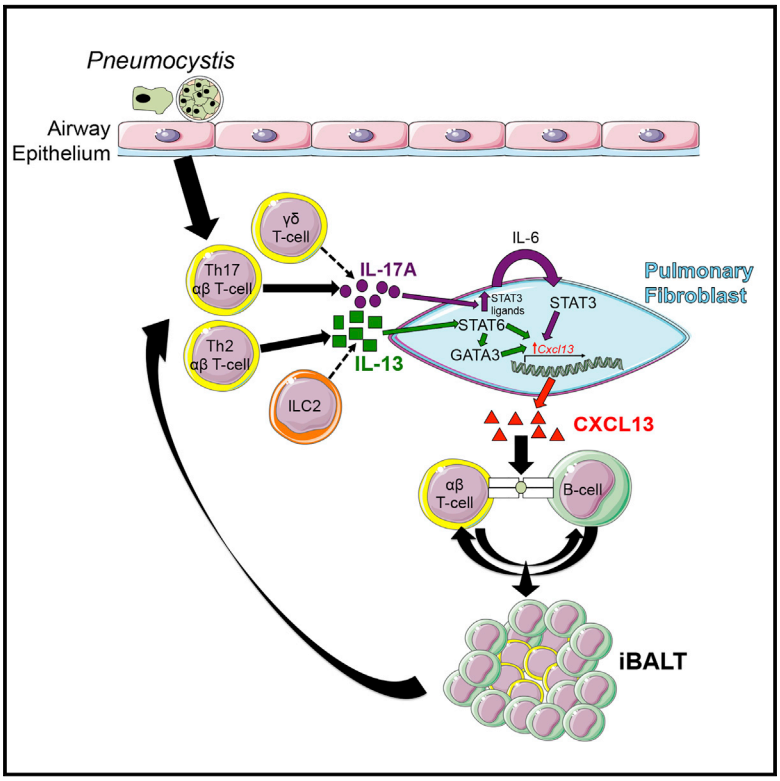

Authors

Taylor Eddens, Waleed Elsegeiny, Maria de la Luz Garcia-Hernadez, ..., Kong Chen, Javier Rangel-Moreno, Jay K. Kolls

Correspondence

jay.kolls@chp.edu

In Brief

Eddens et al. develop a model for fungal-inducible bronchus-associated lymphoid tissue (iBALT) formation driven by infection or exposure to *Pneumocystis*. *Pneumocystis* induces Th2 and Th17 immunity, both of which are required for iBALT formation.

Highlights

- *Pneumocystis* infection results in development of iBALT in a CXCL13-dependent manner
- *Pneumocystis*-driven iBALT formation requires both Th2 and Th17 immunity
- Pulmonary fibroblasts treated with IL-13 and IL-17A synergistically induce *Cxcl13*
- IL-17A/IL-13 stimulation requires STAT3, STAT6, and GATA3 for induction of *Cxcl13*

Eddens et al., 2017, Cell Reports *18*, 3078–3090
March 28, 2017
http://dx.doi.org/10.1016/j.celrep.2017.03.016

OPEN ACCESS
CellPress

Cell Reports
Article

Pneumocystis-Driven Inducible Bronchus-Associated Lymphoid Tissue Formation Requires Th2 and Th17 Immunity

Taylor Eddens,[1] Waleed Elsegeiny,[1] Maria de la Luz Garcia-Hernadez,[2] Patricia Castillo,[1] Giraldina Trevejo-Nunez,[1] Katelin Serody,[1] Brian T. Campfield,[3] Shabaana A. Khader,[4] Kong Chen,[1] Javier Rangel-Moreno,[5] and Jay K. Kolls[1,6,*]

[1]Richard King Mellon Foundation Institute for Pediatric Research, Children's Hospital of Pittsburgh of UPMC, Pittsburgh, PA 15224, USA
[2]Aab Cardiovascular Research Institute, Department of Medicine, University of Rochester, Rochester, NY 14624, USA
[3]Division of Pediatric Infectious Diseases, Department of Pediatrics, University of Pittsburgh School of Medicine, Pittsburgh, PA 15224, USA
[4]Department of Molecular Microbiology, Washington University School of Medicine, St. Louis, MO 63110, USA
[5]Department of Medicine, Allergy/Immunology, and Rheumatology, University of Rochester, Rochester, NY 14624, USA
[6]Lead contact
*Correspondence: jay.kolls@chp.edu
http://dx.doi.org/10.1016/j.celrep.2017.03.016

SUMMARY

Inducible bronchus-associated lymphoid tissue (iBALT) is an ectopic lymphoid structure composed of highly organized T cell and B cell zones that forms in the lung in response to infectious or inflammatory stimuli. Here, we develop a model for fungal-mediated iBALT formation, using infection with *Pneumocystis* that induces development of pulmonary lymphoid follicles. *Pneumocystis*-dependent iBALT structure formation and organization required CXCL13 signaling. *Cxcl13* expression was regulated by interleukin (IL)-17 family members, as *Il17ra*$^{-/-}$, *Il17rb*$^{-/-}$, and *Il17rc*$^{-/-}$ mice failed to develop iBALT. Interestingly, *Il17rb*$^{-/-}$ mice have intact Th17 responses, but failed to generate an anti-*Pneumocystis* Th2 response. Given a role for Th2 and Th17 immunity in iBALT formation, we demonstrated that primary pulmonary fibroblasts synergistically upregulated *Cxcl13* transcription following dual stimulation with IL-13 and IL-17A in a STAT3/GATA3-dependent manner. Together, these findings uncover a role for Th2/Th17 cells in regulating *Cxcl13* expression and provide an experimental model for fungal-driven iBALT formation.

INTRODUCTION

Inducible bronchus-associated lymphoid tissues (iBALT) are ectopic lymphoid structures that form in the lung in response to a variety of infectious stimuli (Foo and Phipps, 2010; Pitzalis et al., 2014). iBALT structures mirror the organization of secondary lymphoid organs (SLO), as both have distinctive T and B cell zones with proliferating lymphocytes (Cyster, 2003; Foo and Phipps, 2010; Randall, 2010). iBALT has been shown previously to provide enhanced protection and confer increased survival to influenza in mice lacking SLOs (Moyron-Quiroz et al., 2004, 2006). Several key soluble mediators implicated in SLO development also have critical roles in iBALT formation. Members of the homeostatic chemokine family, CXCL13 (a ligand for CXCR5) and CCL19/CCL21 (ligands for CCR7) have been shown to facilitate iBALT organization (Cyster, 2003; Kocks et al., 2007; Rangel-Moreno et al., 2006). Interestingly, despite production by dendritic cells, these chemokines appear to be predominantly produced by local pulmonary non-hematopoietic cell populations in response to influenza (GeurtsvanKessel et al., 2009; Rangel-Moreno et al., 2007).

Two other factors, lymphotoxin-alpha (LTα) and interleukin (IL)-17A, have been implicated previously as upstream drivers of *Cxcl13* expression. Mice deficient in LTα fail to develop SLOs, have a disorganized splenic architecture, and likewise have unorganized iBALT structures (Moyron-Quiroz et al., 2004, 2006; De Togni et al., 1994). LTα and CXCL13 are part of a positive feedback loop, where CXCL13 signaling through CXCR5 induces LTα, while LTα signaling through LT-βR induces more CXCL13 (Bracke et al., 2013; Litsiou et al., 2013). Additionally, it has been previously shown that IL-17A is required for iBALT formation using a neonatal LPS/influenza challenge models (Rangel-Moreno et al., 2011). Furthermore, neonatal pulmonary fibroblasts treated with IL-17A upregulate expression of *Cxcl13* (Rangel-Moreno et al., 2011). The finding that iBALT forms more easily in neonate mice appears to have a human correlate, as infants and young children have iBALT structures at a higher frequency than healthy adults (Emery and Dinsdale, 1973; Tschernig et al., 1995). However, patients with conditions associated with chronic pulmonary inflammation (e.g., asthma, chronic obstructive pulmonary disease) appear to promote iBALT formation (Elliot et al., 2004; John-Schuster et al., 2014).

Pneumocystis jirovecii remains a common opportunistic infection in patients with immunodeficiencies (e.g., genetic or AIDS) or receiving immunosuppressive drug regimens as therapy (e.g., autoimmune conditions, hematologic malignancy, post-transplantation rejection) (Eddens and Kolls, 2015; Maini et al., 2013; Mikaelsson et al., 2006; Morris et al., 2004a). However, the ubiquitous nature of *Pneumocystis* exposure in the

immunocompetent population may also have pathologic consequences. For example, one study found that the majority of healthy children by the age of 6 had detectable anti-*Pneumocystis* antibodies (Respaldiza et al., 2004). Furthermore, using molecular techniques, Vargas et al. (2013) demonstrated that nearly all infants by the age of 3 months had *Pneumocystis* present in their lungs. Colonization with *Pneumocystis* in these infants was associated with increases in a chloride channel associated with mucus release, suggestive of potential pathologic response to the fungus (Pérez et al., 2014). Likewise, we have previously demonstrated that *Pneumocystis* exposure in mice led to asthma-like pathology, and a subset of patients with severe asthma had increased antibody responses against *Pneumocystis* (Eddens et al., 2016).

Given the previous findings connecting asthma to *Pneumocystis*, as well as asthma to iBALT, we sought to examine a potential relationship between *Pneumocystis* and iBALT formation. Here, we demonstrate that infection and exposure with *Pneumocystis* induces a protective, robust formation of iBALT in a CXCL13-dependent manner, while LTα was required for germinal center development. Furthermore, both Th2 and Th17 cells induced by *Pneumocystis* infection were required for optimal *Cxcl13* induction and iBALT formation. Finally, we demonstrate that IL-17A and IL-13 synergistically regulate *Cxcl13* expression in pulmonary fibroblasts using a STAT3- and GATA3-dependent pathway, respectively.

RESULTS

Inducible Bronchial-Associated Lymphoid Tissue Develops following *Pneumocystis* Infection and Exposure

Over the course of murine *Pneumocystis* infection, we observed small but distinctive perivascular lymphocytic accumulations with an iBALT appearance at day 7 post-infection (Figure 1A). These ectopic structures continued expanding by day 14 post-infection and subsequently contracted by day 28 (Figure 1A). The lymphocytic follicles were equipped with peripheral node addressin$^+$ (PNAd$^+$) high endothelial venules outside the lymphoid follicles, which are likely supporting attraction and recirculation of CD62L$^+$ naive and central memory T cells (Figure 1B). Furthermore, lymphatic vessel endothelial hyaluronan receptor 1 (Lyve-1$^+$) lymphatic vessels were also present in the surrounding areas of the follicle (Figure 1B). Importantly the formation of iBALT following *Pneumocystis* infection was not an artifact of oropharyngeal infection with a large inoculum. C57BL/6 mice co-housed with a *Pneumocystis* infected *Rag2*$^{-/-}$*Il2rg*$^{-/-}$ double knockout mouse for 2 weeks also had formation of perivascular follicles 4 weeks post-exposure (Figure 1C). Formation of iBALT following co-housing required adaptive immunity, as *Rag1*$^{-/-}$ mice did not have lymphoid follicles following co-housing (Figure 1C). Interestingly, both C57BL/6 and *Rag1*$^{-/-}$ mice co-housed with an infected *Rag2*$^{-/-}$*Il2rg*$^{-/-}$ mouse had detectable *Pneumocystis* burden 4 weeks removed from exposure, confirming both the aerial transmission and sustained infection by *Pneumocystis* (Figure 1D).

We next sought to characterize the lymphoid populations contained within the structures. A classic cellular component of iBALT structures are B cells that are progressively experiencing changes in their phenotype, ranging from small naive B cells to more activated large proliferating germinal center B cells. In C57BL/6 mice inoculated with *Pneumocystis* oropharyngeally, iBALT structures contained large, proliferating cell nuclear antigen (PCNA)-positive BB20^{Lo} B cell blasts as well as inter- and intra-follicular CD3$^+$ T cells (Figure 1E). Although PNA non-specifically binds to carbohydrates found within the alveolar spaces, large PNA$^+$B220^{Lo} blasts are present within germinal centers (Figures 1E and S1). CD4$^+$ T cells are crucial for the development of these structures, as depletion with an anti-CD4 monoclonal antibody (GK1.5) completely abrogated the organization of the B cell follicles and impaired the accumulation and proliferation of activated B cells (Figure 1F). Likewise, depletion of B cells with an anti-CD20 monoclonal antibody (5D2) disrupted organization in the iBALT structures (Figure 1G). Morphometric analysis of these iBALT structures demonstrated that both CD4$^+$ and CD20$^+$ depletion resulted in the reduction of lymphoid follicle size, number, and area occupied per lung section (Figure 1H).

Fungal exposure of any species was not sufficient to induce iBALT, as *Aspergillus*-infected mice did not have lymphoid follicles in the lung 14 days post-infection (Figure S2A). At this time point, *Aspergillus* burden was undetectable, as were any residual inflammatory changes (Figure S2B). Together, these results suggest that *Pneumocystis* may be a unique fungal pathogen capable of stimulating iBALT formation as a result of unique molecular patterns or the chronicity of the infection.

Effector CD4$^+$ T Cells from iBALT Structures Provide Protection against *Pneumocystis* Infection

To define the protective role of the iBALT structures in our model, CD4$^+$ T cells were isolated from the lung, the mediastinal lymph node (mLN), and spleen at day 14 post-infection and were adoptively transferred into a *Pneumocystis*-infected *Rag1*$^{-/-}$ mouse (Figure 2A). Fourteen days following transfer, CD4$^+$ T cells from the spleen, mLN, and iBALT structures were all capable of reducing *Pneumocystis* burden by 10-fold compared to no transfer controls (Figure 2B). Transferred splenic, mLN, and iBALT CD4$^+$ T cells significantly induced transcription of effector cytokines such as *Ifng*, *Il13*, and *Il17a* within the lung (Figure 2C). Interestingly, mLN appeared to have the highest transcription of *Il13*, while production of *Ifng* and *Il17a* was similar among groups (Figure 2C). These results demonstrate that like other conventional T cell populations in the spleen and mLN, iBALT CD4$^+$ T cells are capable of providing protection against *Pneumocystis* infection.

Lymphotoxin-alpha and CXCL13 Are Required for *Pneumocystis*-Driven iBALT Maturation

Lymphotoxin-alpha (LTα) has been previously implicated as an upstream mediator in the production of homeostatic chemokines that are critical in iBALT formation in response to influenza infection (Rangel-Moreno et al., 2011) and as an inducer of *Cxcl13* production following smoke exposure in mice (Demoor et al., 2009). In *Lta*$^{-/-}$ mice infected with *Pneumocystis*, the cellular characterization of iBALT structures by immunofluorescence showed small proliferating B cells and lacked

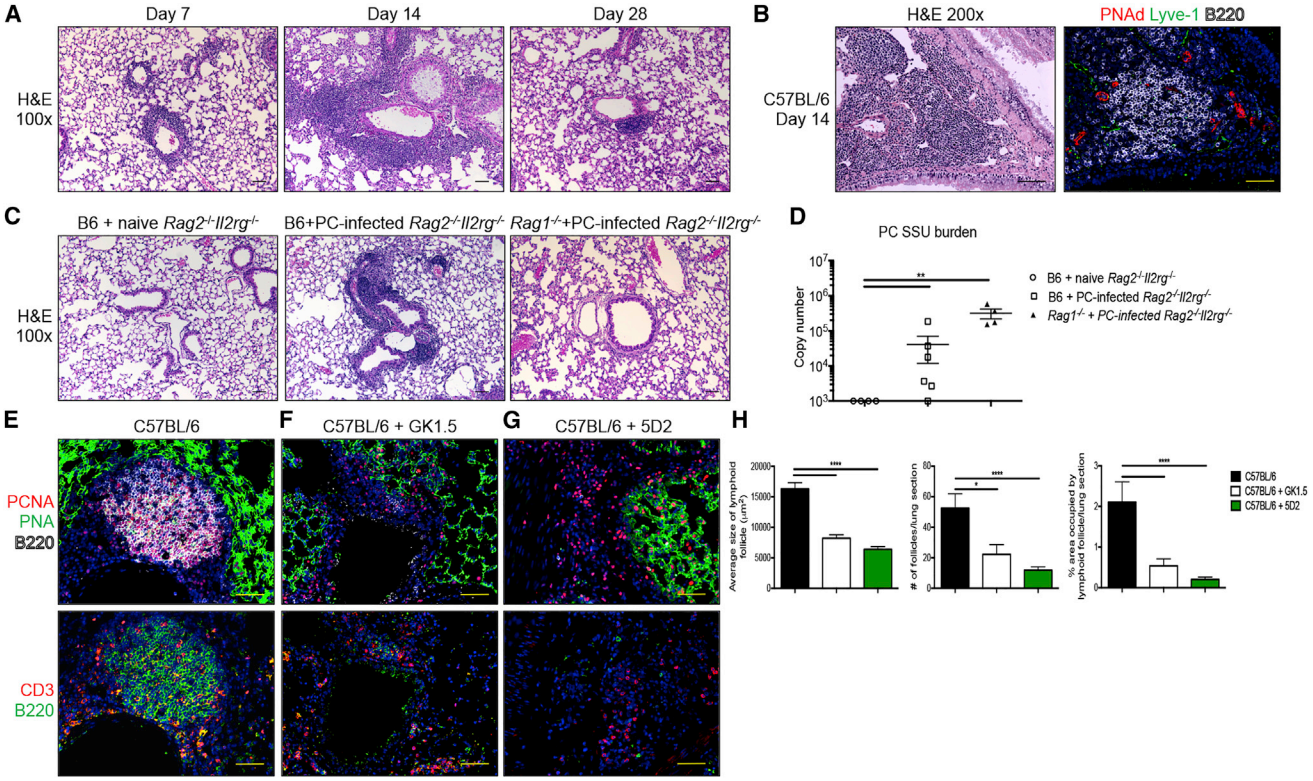

Figure 1. Inducible Bronchus-Associated Lymphoid Tissue Forms following *Pneumocystis* Infection and Exposure

(A) Inducible bronchus-associated lymphoid tissue (iBALT) development over the course of *Pneumocystis* infection.

(B) Immunofluorescent staining of an iBALT structure 14 days post-infection with *Pneumocystis* demonstrating the presence of PNAd$^+$ high endothelial venules and Lyve-1$^+$ lymphatic vessels.

(C) C57BL/6 mice co-housed for 2 weeks with a *Pneumocystis* infected *Rag2*$^{-/-}$*Il2rg*$^{-/-}$ mouse have iBALT structures 4 weeks following separation, while similarly co-housed *Rag1*$^{-/-}$ mice do not.

(D) C57BL/6 and *Rag1*$^{-/-}$ mice co-housed for 2 weeks with a *Pneumocystis* infected *Rag2*$^{-/-}$*Il2rg*$^{-/-}$ mouse have detectable *Pneumocystis* burden.

(E) Immunofluorescent staining of rapidly dividing B cells (PCNA$^+$B220$^+$) cells and CD3$^+$ T cells in the lung of a C57BL/6 mouse 14 days after *Pneumocystis* infection.

(F) iBALT structures are reduced following CD4$^+$ T cell depletion with GK1.5 monoclonal antibody.

(G) iBALT structures are reduced following CD20$^+$ B cell depletion with 5D2 monoclonal antibody. Scale bars, 100 μm.

(H) Quantification of iBALT structures in C57BL/6 mice, C57BL/6 mice treated with GK1.5, and C57BL/6 mice treated with 5D2 (n = 4 per group). Data are shown as mean ± SEM. *p < 0.05, **p < 0.01, ****p < 0.0001 by one-way ANOVA with Tukey's multiple comparisons.

PCNA$^+$B220^{lo} germinal center B cells compared to C57BL/6 mice (Figure 3A). Additionally, we detected infiltrating CD4$^+$ T cells within the disorganized follicles in *Lta*$^{-/-}$ mice (Figure 3B). Despite the lack of functional organization, iBALT structures in *Lta*$^{-/-}$ mice were larger, more numerous, and consumed more area of lung parenchyma compared to C57BL/6 mice (Figure 3C). Unexpectedly, despite the interruption of the positive feedback loop between homeostatic chemokines and LTα, *Lta*$^{-/-}$ mice had comparable levels of *Cxcl13* production compared to C57BL/6 mice (Figure 3D). T cell responses, as measured by *Pneumocystis*-specific interferon (IFN)-γ, IL-5, and IL-17A production, were preserved in *Lta*$^{-/-}$ mice (Figure S3A). However, consistent with the lack of germinal centers, *Lta*$^{-/-}$ mice had defective anti-*Pneumocystis* IgG in the serum, comparable to that of CD4$^+$ T cell-depleted mice (Figure 3E). Despite defective humoral immunity, *Lta*$^{-/-}$ mice were still able to clear *Pneumocystis* at day 14 post-infection like C57BL/6 mice (Figure 3F).

Much like LTα, ligands for both CXCR5 (CXCL13) and CCR7 (CCL19 and CCL21) have previously been implicated in the formation and compartmentalization of secondary lymphoid organ and iBALT formation in both mice and humans (Bracke et al., 2013; GeurtsvanKessel et al., 2009; Rangel-Moreno et al., 2007). Over the course of *Pneumocystis* infection, *Cxcl13*, but not *Ccl19* or *Ccl21*, was induced in a concomitant manner to iBALT formation (Figure 4A) Importantly, *Cxcl13* induction was absent in GK1.5-treated mice, suggesting CD4$^+$ T cells regulate expression of this chemokine (Figure 4A). Likewise, C57BL/6 wild-type mice that developed iBALT following exposure to a *Pneumocystis*-infected *Rag2*$^{-/-}$*Il2rg*$^{-/-}$ mouse had increased *Cxcl13*, but not *Ccl19* or *Ccl21* expression (Figure 4B). Cells of the adaptive immune system were also required for optimal *Cxcl13* expression following co-housing with a *Pneumocystis*-infected *Rag2*$^{-/-}$*Il2r*$^{-/-}$ mouse, as co-housed *Rag1*$^{-/-}$ mice failed to upregulate the chemokine

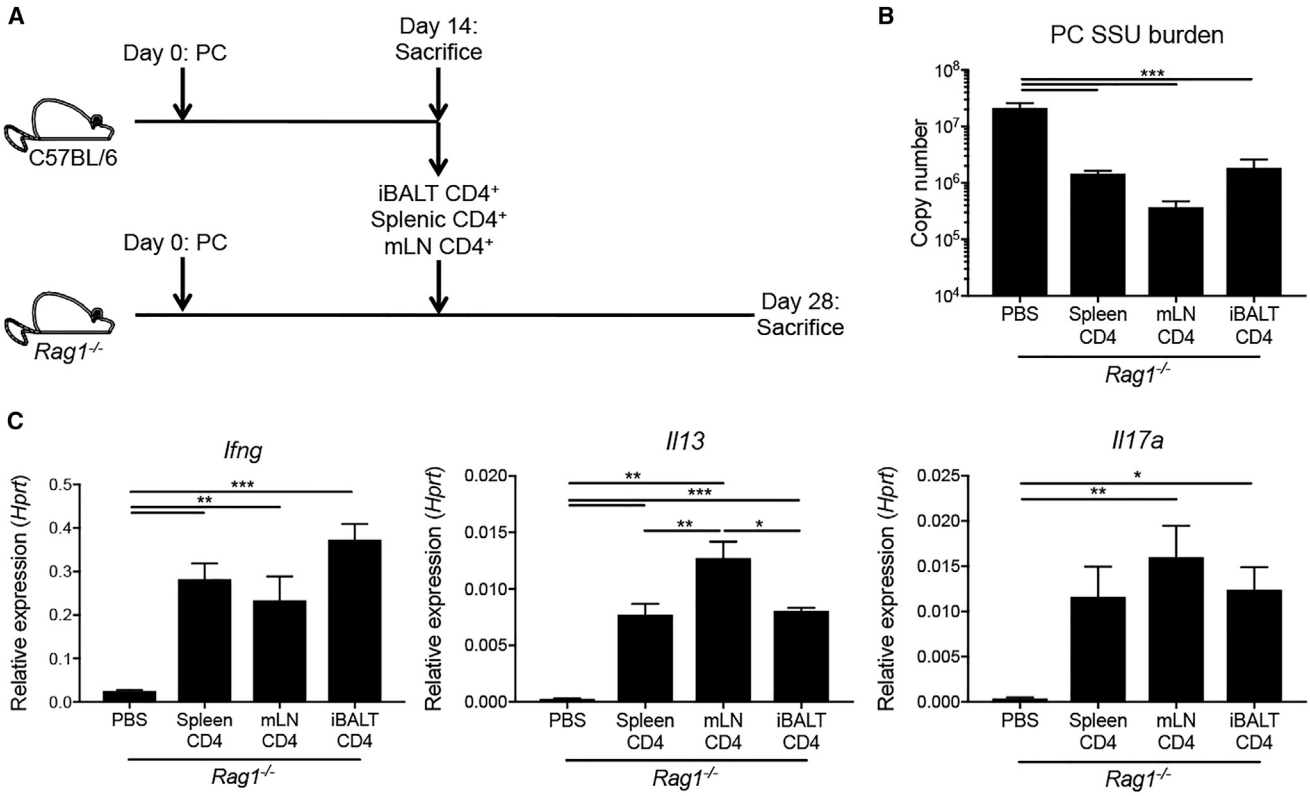

Figure 2. CD4$^+$ T Cells from the Spleen, Mediastinal Lymph Node, and iBALT Structures Are Protective against *Pneumocystis* Infection

(A) Schematic representation of isolation of spleen, mediastinal lymph node (mLN), and iBALT CD4$^+$ T cells at day 14 post-*Pneumocystis* infection, followed by adoptive transfer into a previously infected *Rag1*$^{-/-}$ mouse.

(B) Transfer of splenic, mLN, and iBALT CD4$^+$ T cells reduces *Pneumocystis* burden compared to no transfer (PBS) control.

(C) Expression of *Ifng*, *Il13*, and *Il17a* in whole lung following transfer of CD4$^+$ T cells from spleen, mLN, and iBALT demonstrating preserved effector function in each population. Data are shown as mean ± SEM. *p < 0.05, **p < 0.01, ***p < 0.001 by one-way ANOVA with Tukey's multiple comparisons.

(Figure 4B). Further implicating CXCL13 as a crucial mediator of *Pneumocystis* iBALT formation and organization, *Cxcr5*$^{-/-}$ mice lacked organized follicles containing T cell and B cells zones in the lung 14 days post-infection (Figure 4C). Consistent with the key role for CXCL13 in the attraction of CXCR5$^+$ B cells, there were very few B cells within the follicles in IBALT areas of *Cxcr5*$^{-/-}$ mice (Figure 4D). Interestingly, despite the paucity of organization in *Cxcr5*$^{-/-}$ mice, the size, number, and area consumed by inflammatory infiltrates were comparable to that of C57BL/6 mice (Figure 4E). Surprisingly, despite the lack of draining lymph nodes and the presence of poorly organized iBALT structures, *Cxcr5*$^{-/-}$ mice had an intact humoral immune response and produced anti-*Pneumocystis* IgG (Figure S3B). However, CD4$^+$ T cells from the lungs of *Cxcr5*$^{-/-}$ mice had greater *Pneumocystis*-specific IFN-γ and impaired production of IL-5 compared to C57BL/6 mice (Figure S3C). Despite subtle changes in T cell phenotype, *Cxcr5*$^{-/-}$ mice were capable of clearing *Pneumocystis* infection by day 14 post-infection (Figure 4F). Together, these findings demonstrate a role for LTα and CXCR5 in germinal center formation and iBALT organization, independently of the induction of protective pulmonary immunity against *Pneumocystis*.

Pneumocystis iBALT Is Dependent on CD4$^+$ Th2 and Th17 Cells

As the observed increase in *Cxcl13* expression was CD4$^+$ T cell-dependent, we next characterized the T-helper responses to *Pneumocystis* infection at day 7 post-infection, prior to significant *Cxcl13* mRNA induction. Mice infected with *Pneumocystis* had significant increases in both IL-17A and IL-13 single-producing, as well as IL-17A$^+$IL-13$^+$ double-producing αβ CD4$^+$ T cells compared to naive controls (Figures S4A–S4D). Innate lymphoid cells and γδ T cells appeared to be minor contributors of both IL-17A and IL-13 (Figures S4A–S4C). Likewise, at day 7 post-infection, no significant induction of *Il17a* and *Il13* transcript was noted in *Rag1*$^{-/-}$ or *Rag2*$^{-/-}$*Il2rg*$^{-/-}$ mice, further confirming the predominant role of T-helper cells as cytokine producers (Figure S4E). The hallmark cytokine of Th1 cells, interferon-γ, was only modestly induced (data not shown).

Additionally, at day 14 post-infection, αβ CD4$^+$ T cells greatly outnumbered both innate lymphoid cells and γδ T cells in the lungs (Figure S4F). Furthermore, γδ T cells appeared to be secondary contributors to iBALT formation, as *Tcrd*$^{-/-}$ mice developed large lymphoid follicles at day 14 post-infection (Figure S4G). Together, these findings suggest that Th2 and Th17 cells accumulate in the lung following *Pneumocystis* infection

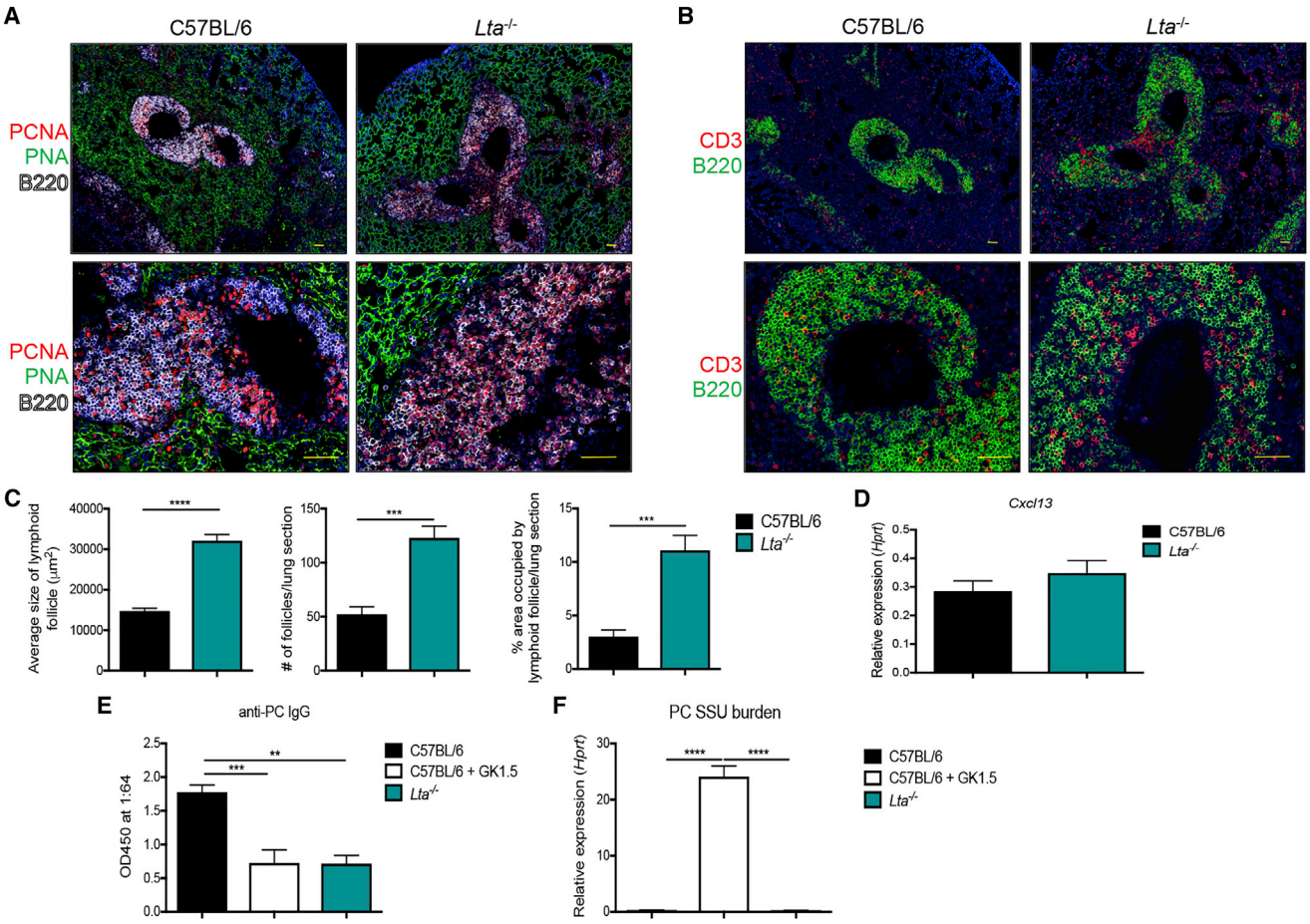

Figure 3. Lymphotoxin-alpha Is Required for iBALT Organization and Germinal Center Development following *Pneumocystis* Infection

(A) Immunofluorescent staining of C57BL/6 and $Lta^{-/-}$ mice 14 days following *Pneumocystis* infection demonstrating a lack of $PCNA^{+}B220^{lo}$ germinal center B cells in $Lta^{-/-}$ mice compared to C57BL/6 mice. Scale bars, 100 μm.

(B) Immunofluorescent staining of C57BL/6 and $Lta^{-/-}$ mice demonstrating intrafollicular $CD3^{+}$ T cells. Scale bars, 100 μm.

(C) Quantification of size, number, and area occupied by iBALT structures (n = 7–8). ***p < 0.001, ****p < 0.0001 by Student's t test.

(D) Expression of *Cxcl13* is similar between C57BL/6 and $Lta^{-/-}$ mice in whole lung (n = 7).

(E) $Lta^{-/-}$ mice have deficient production of serum anti-*Pneumocystis*-specific IgG compared to C57BL/6 mice (n = 4–6).

(F) $Lta^{-/-}$ mice sufficiently clear *Pneumocystis* infection comparable to that of C57BL/6 controls (n = 3–7). Data are shown as mean ± SEM. **p < 0.01, ***p < 0.001, ****p < 0.0001 by one-way ANOVA with Tukey's multiple comparisons.

and are the primary cytokine producers starting at day 7 post-infection.

Given the robust Th17 response, we next evaluated the contribution of IL-17 receptor family members, IL-17RA, IL-17RB, and IL-17RC, in *Pneumocystis*-driven iBALT formation. IL-17A signals through a heterodimeric complex of IL-17RA and IL-17RC, while the Th2-promoting cytokine IL-25 (IL-17E) signals through IL-17RA and IL-17RB (Gaffen, 2009; Rickel et al., 2008). IL-17A has been previously implicated in triggering both *Cxcl13* production and iBALT formation after LPS instillation into neonatal mice and during experimental infection with influenza viruses and *Mycobacterium tuberculosis* (Gopal et al., 2013; Rangel-Moreno et al., 2011). Similar to those models, *Pneumocystis*-driven iBALT was disrupted in $Il17ra^{-/-}$ mice compared to wild-type controls, as $Il17ra^{-/-}$ mice had drastic reductions in $PCNA^{+}$-$B220^{+}$ cells and showed little organization in iBALT structures (Figure 5A). Surprisingly, iBALT formation was severely compromised in $Il17rb^{-/-}$ mice following *Pneumocystis* infection (Figure 5A). Likewise, $Il17rc^{-/-}$ mice had a reduction in iBALT size and poor cellular organization (Figure 5A). Upon quantification, $Il17ra^{-/-}$, $Il17rb^{-/-}$, and $Il17rc^{-/-}$ mice all had significantly reduced follicle number and average size, as well as area occupied within the lung (Figure 5B). In concordance with the histologic data, $Il17ra^{-/-}$, $Il17rb^{-/-}$, and $Il17rc^{-/-}$ mice had reduced expression of *Cxcl13* in the infected lung (Figure 5C). Consistent with a role for IL-25 in type II immune responses, $Il17ra^{-/-}$ and $Il17rb^{-/-}$ mice both had diminished expression of *Il5 and Il13* expression and IL-4 production following ex vivo stimulation with *Pneumocystis* antigen (Figures S5A and S5B). $Il17rc^{-/-}$ mice had Th2 cytokine expression and production comparable to that of C57BL/6 mice, suggestive of intact Th2 priming and differentiation (Figures S5A and S5B). Production of *Il17a*

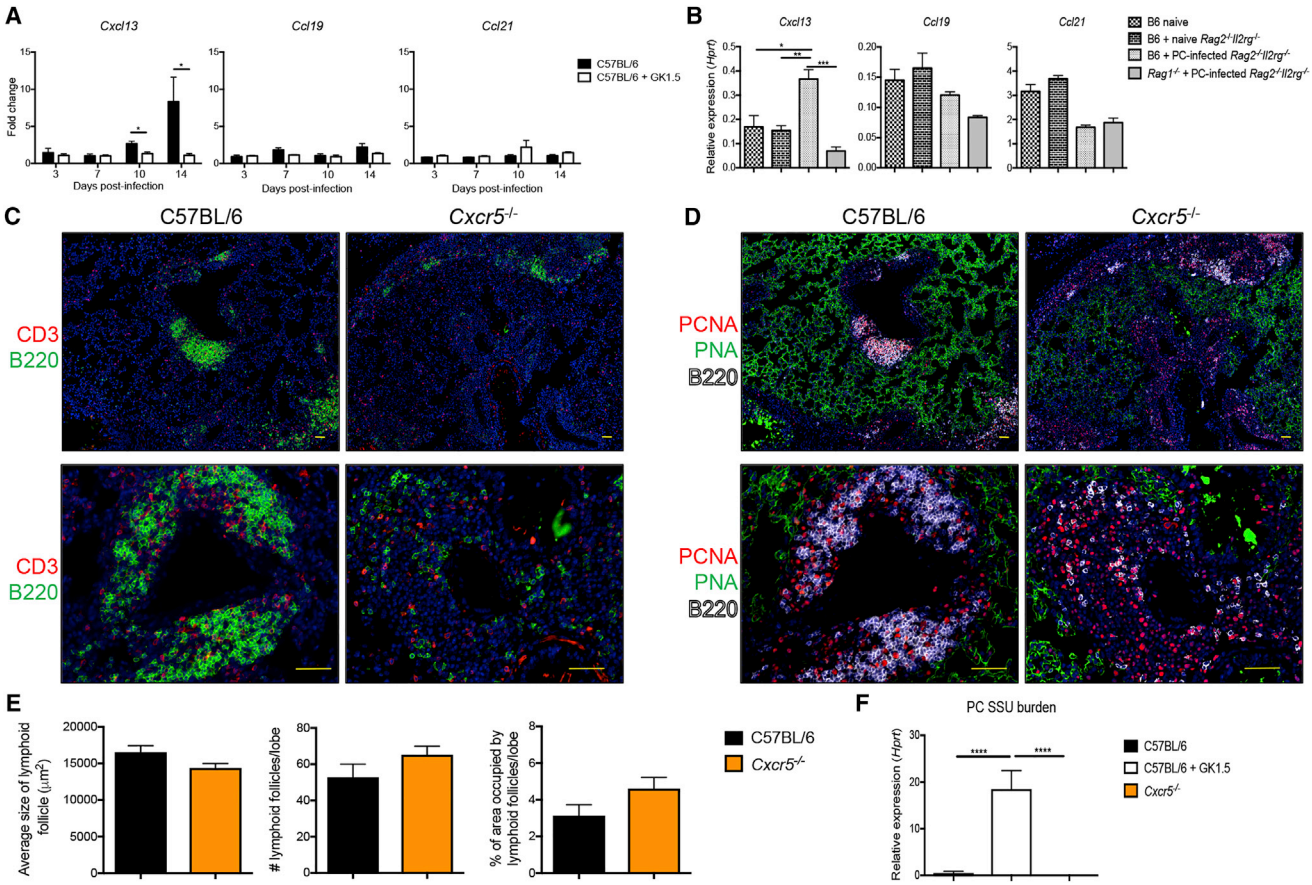

Figure 4. CXCR5 Signaling Is Required for *Pneumocystis* iBALT Formation

(A) *Cxcl13* is induced over the course of *Pneumocystis* infection in C57BL/6 mice in a $CD4^+$ T cell-dependent manner. *Ccl19* and *Ccl21* expression levels are unchanged throughout *Pneumocystis* infection. *p < 0.05 by multiple t tests, (n = 5 per group).

(B) C57BL/6 mice co-housed with a *Pneumocystis* infected $Rag2^{-/-}Il2rg^{-/-}$ mouse for 2 weeks, followed by 4 weeks of separation, upregulate *Cxcl13* but not *Ccl19* or *Ccl21* (n = 3–6 per group). *p < 0.05, **p < 0.01, ***p < 0.001 by one-way ANOVA with Tukey's multiple comparisons.

(C) Immunofluorescent staining of $Cxcr5^{-/-}$ mice shows disorganized follicles lacking T cell and B cell zones compared to C57BL/6 mice following *Pneumocystis* infection. Scale bars, 100 μm.

(D) $Cxcr5^{-/-}$ mice have disorganized B cell follicle structure after *Pneumocystis* infection compared to C57BL/6 mice. Scale bars, 100 μm.

(E) Quantification of size, number, and area occupied by lymphocytic infiltrates (n = 7–8).

(F) C57BL/6 (n = 10) and $Cxcr5^{-/-}$ (n = 4) control *Pneumocystis* burden at 14 days post-infection compared to CD4-depleted mice (n = 6). Data are shown as mean ± SEM. ***p < 0.001, ****p < 0.0001 by one-way ANOVA with Tukey's multiple comparisons.

and *Ifng* was largely unchanged among the various genotypes (Figure S5A).

As both $Il17ra^{-/-}$ and $Il17rb^{-/-}$ mice had reduced lymphoid follicle development and defective Th2 responses, we next sought to confirm the role of the IL-17RB ligand, IL-25, in iBALT formation. C57BL/6 mice were treated with an anti-IL25 monoclonal antibody prior to fungal infection. At day 14 post-infection with *Pneumocystis*, anti-IL25 treatment substantially reduced lung inflammation, as well as the structural organization of iBALT (Figures S6A and S6B). Both the size and total area occupied by iBALT follicles were also reduced following anti-IL25 treatment, while number of lymphoid follicles was unchanged (Figure S6C). Taken together, these results suggest that $Il17ra^{-/-}$ and $Il17rb^{-/-}$ mice appear to have defective Th2 priming and iBALT formation due to defective IL-25 signaling.

As we have shown previously that eosinophils are a protective downstream mediator of the Th2 response following *Pneumocystis* infection (Eddens et al., 2015), we next examined the expression of the eosinophil marker major basic protein (*Prg2*) in the lungs. Both $Il17ra^{-/-}$ and $Il17rb^{-/-}$ had significantly reduced expression of *Prg2* similar to that of CD4-depleted animals, again demonstrating functional impairment of Th2 responses in these mice (Figure 5D). $Il17rc^{-/-}$ mice, on the contrary, had similar eosinophil recruitment compared to C57BL/6 mice (Figure 5D). Strikingly, $Il17ra^{-/-}$ mice had *Pneumocystis* burden levels comparable to that of CD4-depleted mice suggestive of a synergy between Th2 and Th17 responses, while both $Il17rb^{-/-}$ and $Il17rc^{-/-}$ had trends toward increased burden at day 14 post-infection (Figure 5E).

Further supporting the role of Th2 cells in development of fungal iBALT, $Stat6^{-/-}$ mice had dramatically reduced lymphoid

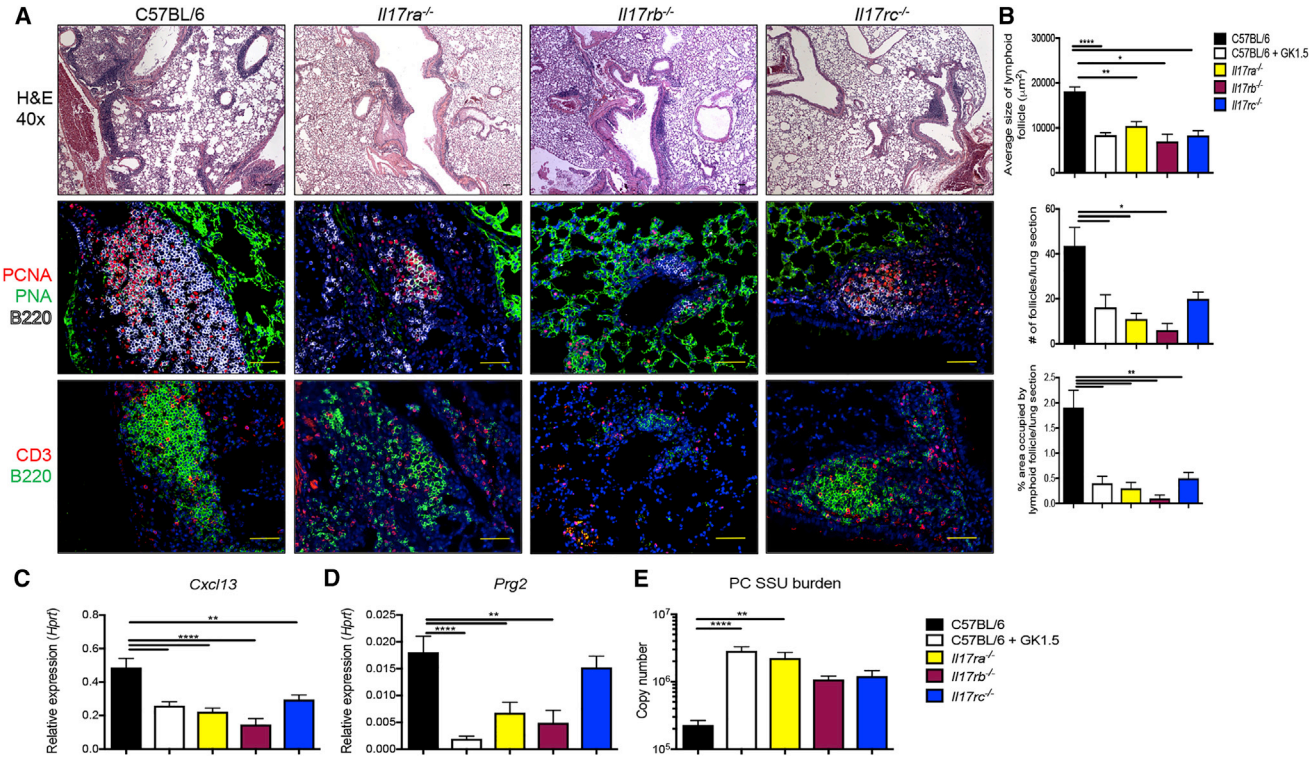

Figure 5. IL-17R Family Members Are Required for the Development of *Pneumocystis* iBALT

(A) Representative immunofluorescent staining of C57BL/6, *Il17ra*$^{-/-}$, *Il17rb*$^{-/-}$, and *Il17rc*$^{-/-}$ mice, respectively, 14 days following *Pneumocystis* infection demonstrates decreased iBALT formation (top). *Il17ra*$^{-/-}$, *Il17rb*$^{-/-}$, and *Il17rc*$^{-/-}$ mice all have reduced proliferating B cells (middle) and disorganized T cell and B cell zones (bottom). Scale bars, 100 μm.

(B) Quantification of size, number, and area occupied by iBALT structures.

(C) *Cxcl13* expression is reduced in whole lung tissue of *Il17ra*$^{-/-}$, *Il17rb*$^{-/-}$, and *Il17rc*$^{-/-}$ mice (n = 8–16).

(D) Eosinophil recruitment as measured by *Prg2* expression is diminished in *Il17ra*$^{-/-}$ and *Il17rb*$^{-/-}$ mice (n = 8–16).

(E) *Il17ra*$^{-/-}$ mice have increased *Pneumocystis* burden comparable to that of CD4-depleted animals, while *Il17rb*$^{-/-}$ and *Il17rc*$^{-/-}$ have a trend toward increased burden (n = 4–12). Data are shown as mean ± SEM. *p < 0.05, **p < 0.01, ****p < 0.0001 by one-way ANOVA with Tukey's multiple comparisons.

follicle development on H&E staining compared to BALB/c controls (Figure S7A). *Stat6*$^{-/-}$ mice had reduced *Il13* mRNA expression compared to BALB/c mice, while *Il17a* transcription levels were similar (Figure S7B). Likewise, C57BL/6 mice treated with a monoclonal antibody against IL-13 had noticeable disruption in iBALT structures compared to controls (Figure S7C). IL-13 neutralization was effective, as measured by the functional ability to block *Muc5ac* expression (Figure S7D). Importantly, IL-13 blockade did not impact transcription of *Il13* or *Il17a* (Figure S7D) but did result in increased *Pneumocystis* burden (Figure S7E). Altogether, these results demonstrate that disruption of either the Th2 or Th17 responses alone was capable of reducing *Pneumocystis* iBALT formation.

Despite the influence of Th2 cells on iBALT formation, eosinophils did not seem to actively participate in the formation of iBALT, as dblGATA1$^{-/-}$ (on a BALB/c background) mice formed lymphoid follicles and expressed *Cxcl13* in a manner similar to that of BALB/c control mice (Figures S7F and S7G). Furthermore, in agreement with previously published data in a sterile *Pneumocystis* antigen model (Eddens et al., 2016), the T cell responses were unperturbed in dblGATA1$^{-/-}$ mice (Figure S7G).

IL-13 and IL-17A Synergistically Induce CXCL13 Production

Formation of *Pneumocystis*-driven iBALT is dependent on CXCL13 production, but surprisingly both mice lacking IL-17 signaling and Th2 cell polarization have defective *Cxcl13* expression. To determine the cellular sources of CXCL13, lung blood endothelial cells (CD45$^-$CD31$^+$podoplanin$^-$), triple negative SLO cells (CD45$^-$CD31$^-$podoplanin$^-$), lymphatic endothelial cells (CD45$^-$CD31$^+$podoplanin$^+$), and pulmonary fibroblasts (CD45$^-$CD31$^-$podoplanin$^+$) were sorted from the lung at day 14 post-infection (Fletcher et al., 2011). All of these cell populations demonstrated significant increases in *Cxcl13* expression, with pulmonary fibroblasts representing the largest relative contributor (Figure 6A). Importantly, the hematopoietic compartment (CD45$^+$) did not increase *Cxcl13* expression following *Pneumocystis* infection (Figure 6A). Pulmonary fibroblasts, as well as the endothelial cells populations, all had high relative expressions of the receptor components for IL-13 (*Il4r* and *Il13ra1*) and IL-17A (*Il17ra* and *Il17rc*) (Figure 6B). To determine the spatial location of CXCL13 producing cells, we performed immunofluorescence in lungs of mice infected with *Pneumocystis*. CXCL13 protein was located within the center of the lymphoid

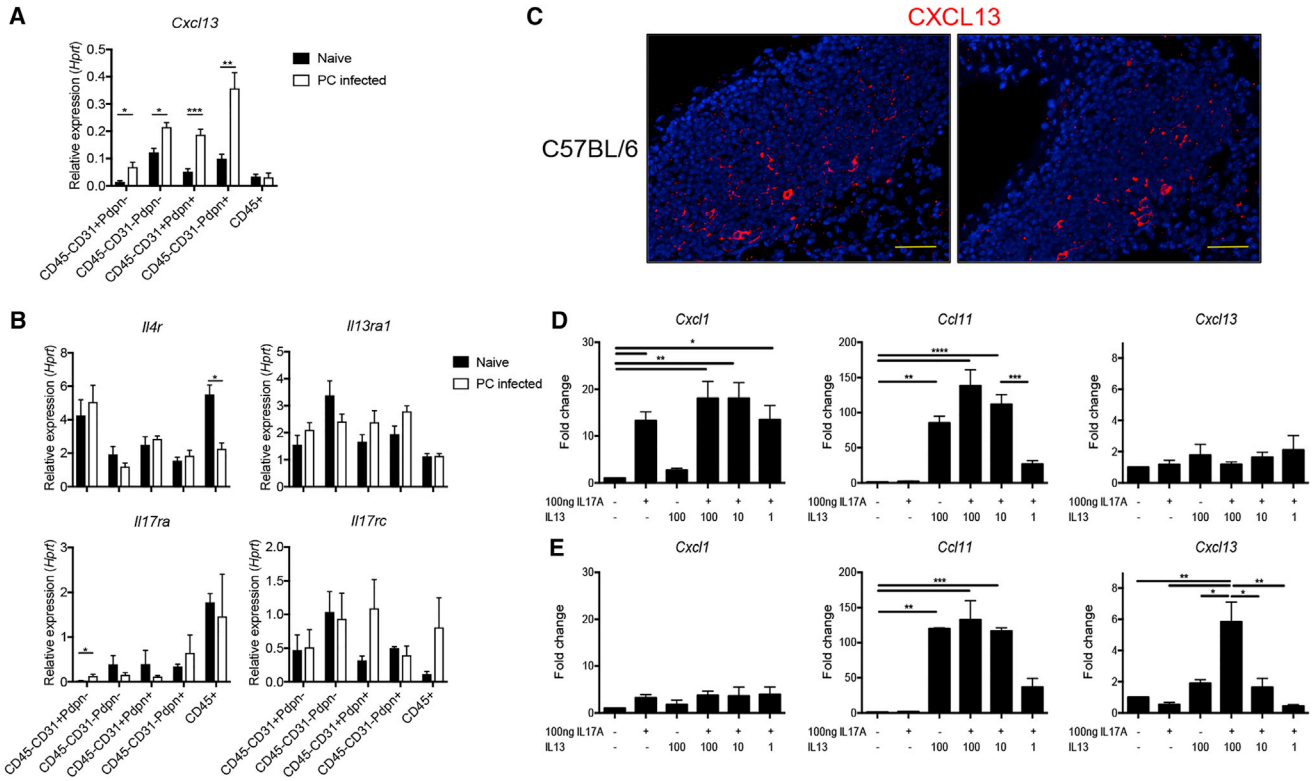

Figure 6. IL-17A and IL-13 Synergistically Regulate *Cxcl13* Expression in Pulmonary Fibroblasts

(A) Expression of *Cxcl13* in sorted lung populations, including CD45$^-$ lung blood endothelial cells (CD31$^+$podoplanin$^-$), triple negative SLO cells (CD31$^-$podoplanin$^-$), lymphatic endothelial cells (CD31$^+$podoplanin$^+$), pulmonary fibroblasts (CD31$^-$podoplanin$^+$), and CD45$^+$ cells at day 14 post-*Pneumocystis* infection (n = 4). *Cxcl13* is induced in the CD45$^-$ cell populations with CD31$^-$podoplanin$^+$ fibroblasts representing the largest relative contributor.

(B) The receptors for IL-13 (*Il4r* and *Il13ra1*) and IL-17A (*Il17ra* and *Il17rc*) are expressed in each cell population. *p < 0.05, **p < 0.01, ***p < 0.001 by Student's t test.

(C) Immunofluorescent staining demonstrates CXCL13 protein within the lymphoid follicle 14 days post-infection with *Pneumocystis*. Scale bars, 100 μm.

(D) Pulmonary fibroblasts upregulate *Cxcl1* and *Ccl11* following a 6-hr stimulation with 100 ng of IL-17A and various doses of IL-13 (in ng), respectively. *Cxcl13* expression is unchanged in all conditions at 6 hr post-stimulation (n = 4).

(E) *Cxcl1* expression is reduced at 24 hr post-stimulation, while *Ccl11* expression persists. Stimulation with both IL-17A and IL-13 leads to upregulation of *Cxcl13* at 24 hr post-stimulation (n = 2–4). Data are shown as mean ± SEM. *p < 0.05, **p < 0.01, ***p < 0.001, ****p < 0.0001 by one-way ANOVA with Tukey's multiple comparisons.

follicles and was undetectable in the airway epithelium and vascular endothelium (Figure 6C). Another known producer of CXCL13, CD21$^+$CD35$^+$FDC-M1$^+$ follicular dendritic cells, were also absent in the *Pneumocystis*-driven follicles (data not shown). These histologic findings, coupled with high *Cxcl13* expression in podoplanin-positive cells, suggest that pulmonary fibroblasts are a primary cellular source of CXCL13.

To that end, we hypothesized that *Cxcl13* expression in pulmonary fibroblasts was being driven by IL-17 and/or the local type II cytokine responses in the lung. Cultured primary pulmonary fibroblasts from adult mice responded to both IL-17A and IL-13 6 hr following stimulation, as the respective conditions led to upregulation of *Cxcl1* and *Ccl11* (Figure 6D). However, *Cxcl13* was not induced 6 hr following stimulation with IL-17A, IL-13, or the combination of the two cytokines (Figure 6D). At 24-hr post-stimulation, *Cxcl13* was significantly upregulated in fibroblasts treated with both IL-17A and IL-13 compared to single stimulation controls (Figure 6E). *Cxcl1* induction at this time point had waned, while *Ccl11* expression remained high in IL-13-treated cells (Figure 6E).

The direct induction of *Cxcl1* by IL-17A coupled with the delayed induction of *Cxcl13*, led us to hypothesize an indirect effect of IL-17A was synergizing with IL-13. Stimulation of pulmonary fibroblasts with IL-17A for 6 hr induced a 4-fold increase in IL-6 production (Figure 7A). Interestingly, IL-6 coupled with IL-13 induced similar levels of *Cxcl13* expression compared to IL-13 and IL-17A co-stimulated cells (Figure 7B). To further demonstrate a role for IL-17A-induced IL-6 in *Cxcl13* mRNA expression, we found that blockade of gp130 attenuated the *Cxcl13* induction following stimulation with IL-17A and IL-13 (Figure 7C). STAT3, a downstream target of IL-6, was required for *Cxcl13* induction, as *Stat3*$^{fl/fl}$ fibroblasts treated with adenovirus-Cre-GFP (Ad-Cre) failed to increase *Cxcl13* transcription with either IL-17A/IL-13 or IL-6/IL-13 stimulation (Figure 7D).

Similarly, canonical IL-13 signaling requires both activation of STAT6 and GATA3. To that end, *Stat6*$^{-/-}$ fibroblasts failed

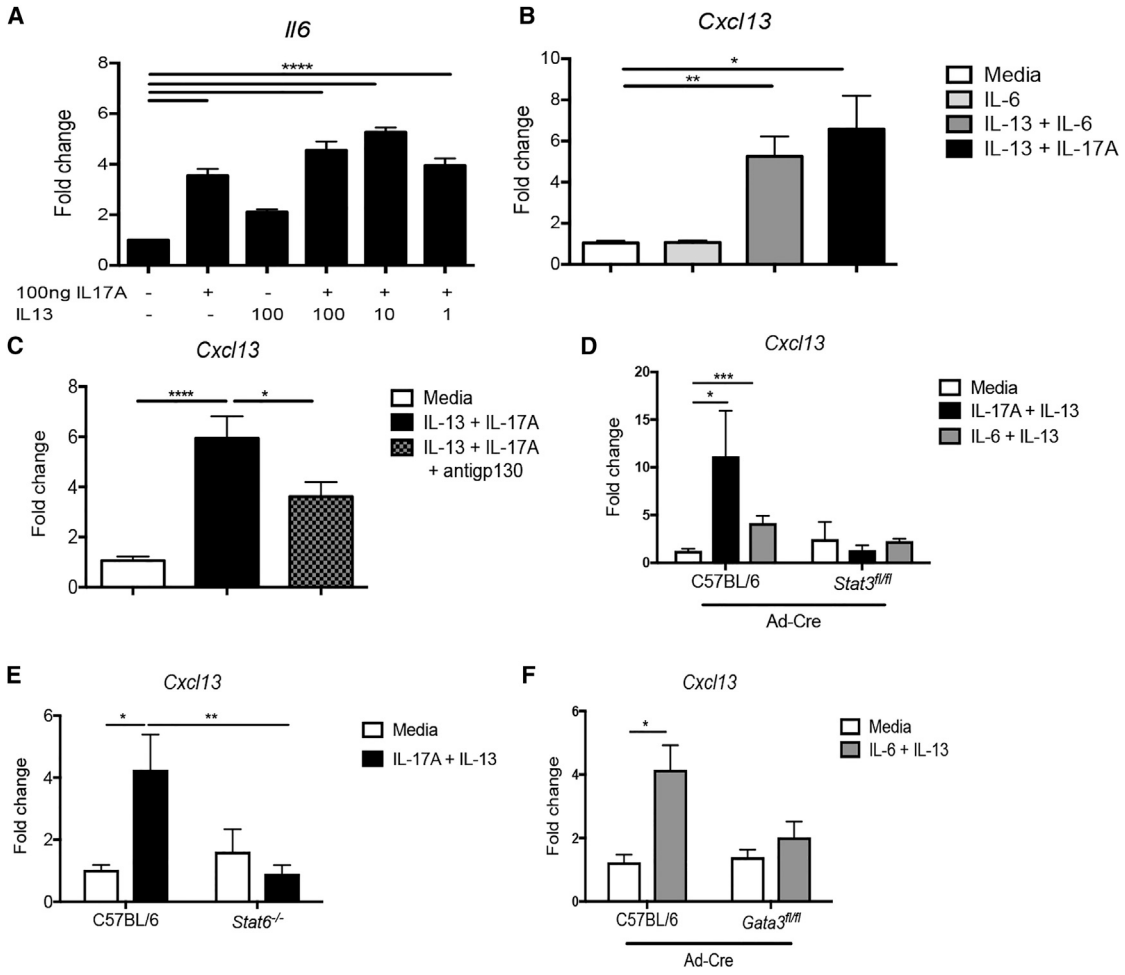

Figure 7. *Cxcl13* Expression Is Dependent on STAT3 and GATA3 Activation

(A) Expression of *Il6* is upregulated in pulmonary fibroblasts following a 6-hr stimulation with IL-17A (n = 4).

(B) *Cxcl13* is induced in pulmonary fibroblast by 24 hr stimulation with IL-13 in combination with either IL-6 or IL-17A (n = 4–10).

(C) *Cxcl13* upregulation is partially blocked by treatment with an anti-gp130 antibody (n = 7–9).

(D) *Cxcl13* expression is attenuated in pulmonary fibroblasts from *Stat3*$^{fl/fl}$ mice following in vitro treatment with adenovirus-Cre (n = 4–12).

(E) *Stat6*$^{-/-}$ fibroblasts fail to upregulate *Cxcl13* following stimulation with IL-17A and IL-13 (n = 3-6).

(F) *Cxcl13* expression is attenuated in pulmonary fibroblasts from *Gata3*$^{fl/fl}$ mice following in vitro treatment with adenovirus-Cre (n = 3–4). Data are shown as mean ± SEM. *p < 0.05, **p < 0.01, ***p < 0.001, ****p < 0.0001 by one-way ANOVA with Tukey's multiple comparisons.

to induce *Cxcl13* following stimulation with IL-17 and IL-13 compared to C57BL/6 controls (Figure 7E). Likewise, *Gata3*$^{fl/fl}$ fibroblasts treated with Ad-Cre did not have upregulation of *Cxcl13* following dual stimulation (Figure 7F). Strikingly, these findings demonstrate an indirect role of IL-17A in activating STAT3 and a direct role of IL-13, STAT6, and GATA3 signaling in inducing *Cxcl13* expression in pulmonary fibroblasts.

DISCUSSION

The current study demonstrates that *Pneumocystis* infection via either oropharyngeal inoculation or natural transmission results in induction of CXCL13 and iBALT formation. Furthermore, the *Pneumocystis*-dependent iBALT structures required signaling through IL-17 family members for optimal iBALT formation/organization, and mice with either defective Th17 or Th2 responses failed to induce CXCL13 expression and develop iBALT. Finally, pulmonary fibroblasts from adult mice stimulated with both IL-17A and IL-13 synergistically upregulate CXCL13 expression in a STAT3- and GATA3-dependent manner.

Importantly, this study identifies a fungal pathogen capable of inducing iBALT. Previously studied models include bacterial (*Pseudomonas*) and viral (influenza, modified vaccinia virus Ankara [MVA]), and subtle differences have begun to emerge in iBALT formation depending on the pathogen of interest (Fleige et al., 2014; GeurtsvanKessel et al., 2009; Halle et al., 2009; Moyron-Quiroz et al., 2004). For example, *Pseudomonas*-driven iBALT formation requires CXCL12-producing stromal cells, while MVA induces iBALT through a CXCL13-producing follicular dendritic cell-dependent mechanism (Fleige et al., 2014). Likewise,

CXCL13 expression has been implicated in influenza-mediated iBALT formation (GeurtsvanKessel et al., 2009; Moyron-Quiroz et al., 2004; Rangel-Moreno et al., 2007). However, unlike MVA infection, CXCL13 expression in response to influenza is mediated primarily by a stromal, and not hematopoietic, source (Rangel-Moreno et al., 2007). Influenza-mediated iBALT requires additionally soluble factors, such as lymphotoxin-alpha, for development. Blockade of the receptor for lymphotoxin-alpha (LTβR) was sufficient to reduce influenza-driven iBALT and neonatal *Lta*$^{-/-}$ mice exposed to LPS followed by a subsequent challenge with influenza failed to develop iBALT (GeurtsvanKessel et al., 2009; Rangel-Moreno et al., 2011). In our model of *Pneumocystis* infection, lymphotoxin-alpha and CXCL13 are required for optimal T and B cell compartmentalization and germinal center formation. These findings further highlight the need to study iBALT in a pathogen-specific manner, as differences in mechanism may arise from unique molecular properties for each pathogen.

Furthermore, despite the requirement for CXCL13 in both the neonatal LPS-influenza and *Pneumocystis* models, the mechanism of *Cxcl13* transcript induction appears to be different. Rangel-Moreno et al. (2011) demonstrated that neonatal pulmonary fibroblasts upregulate *Cxcl13* expression following stimulation with IL-17A. However, in adult pulmonary fibroblasts, IL-17A stimulation does not appear to be sufficient to upregulate *Cxcl13*. Surprisingly, IL-13 and IL-17A, products of the mixed Th2 and Th17 inflammatory response generated by *Pneumocystis*, potently induce *Cxcl13* expression in adult pulmonary fibroblasts. The mechanism of IL-13 and IL-17A synergy appears to be dependent on the hallmark downstream transcription factors, STAT3 and GATA3. These findings suggest that transcriptional regulation of *Cxcl13* is tightened over the course of development, perhaps through epigenetic modifications. Alternatively, it is possible that neonatal fibroblasts have a lower threshold for the activation either STAT3 or GATA3.

Interestingly, STAT3 ligands have been implicated previously in inducing *Cxcl13* expression and initiating iBALT formation. Using transgenic mice expressing both human IL-6 and IL-6R, Goya et al. (2003) were able to elegantly demonstrate that CXCL13-positive lymphoid follicles spontaneously form in the lung. iBALT formation using transgenic lines have not been limited to STAT3 ligands, however. Mice overexpressing IL-5, a Th2 cytokine responsible for eosinophilopoiesis, similarly develop spontaneous iBALT structures in addition to asthma-like pathology (Lee et al., 1997). Of course, these mice recapitulate models of chronic stimulation with each cytokine irrespective of an infectious stimulus.

One unique aspect of this fungal-driven iBALT model is the synergistic nature of both Th17 and Th2 cells over the course of 14 days of infection. Strikingly, mice lacking both IL-17A signaling (*Il17ra*$^{-/-}$ and *Il17rc*$^{-/-}$) and IL-25 signaling (*Il17ra*$^{-/-}$ and *Il17rb*$^{-/-}$) failed to upregulate *Cxcl13* and subsequently develop iBALT. Although IL-17A signaling has previously been implicated in iBALT formation (Gopal et al., 2013; Rangel-Moreno et al., 2011), *Il17rb*$^{-/-}$ mice with intact IL-17A responses, but defective production of *Il5* and *Il13*, failed to form iBALT. Furthermore, blockade of IL-13 signaling in vivo and *Stat6*$^{-/-}$ mice had reduced iBALT formation following *Pneumocystis* infection. Importantly, IL-13 was produced solely by TCRβ^{+} cells and not ILC2s, similar to previous findings in a *Pneumocystis* antigen model (Eddens et al., 2016). Together, these results demonstrate for the first time that Th2 responses participate in iBALT formation synergistically with Th17 cells in response to fungal infection.

While mechanistic studies in the murine model clearly indicate that natural transmission of *Pneumocystis* can induce iBALT formation, the role for *Pneumocystis* in iBALT formation in humans is unknown. Several key populations have been shown previously to develop iBALT: infants (Tschernig et al., 1995), and patients with COPD (John-Schuster et al., 2014; Litsiou et al., 2013), asthma (Elliot et al., 2004), or pulmonary complications of rheumatoid arthritis (Rangel-Moreno et al., 2006). Importantly, colonization of *Pneumocystis* in all of these populations has been documented. Infants are nearly ubiquitously colonized with *Pneumocystis* by the age of 4 months; furthermore, *Pneumocystis* colonization in young children correlates with the increase in a mucus-associated gene, suggestive of a pathologic immune response (Eddens et al., 2016; Pérez et al., 2014; Vargas et al., 2013). Likewise, patients with COPD and *Pneumocystis* have more severe disease and increases in proteases and inflammatory markers (Fitzpatrick et al., 2014; Morris et al., 2004b; Norris and Morris, 2011). While colonization has yet to be fully studied in asthma, a subset of patients with severe asthma have increased anti-*Pneumocystis* IgG and IgE antibodies, which correlates with worsened disease (Eddens et al., 2016). Finally, patients with rheumatoid arthritis can have asymptomatic colonization of *Pneumocystis*, or depending on the therapeutic regimen, can become immunosuppressed enough to develop fulminant *Pneumocystis* pneumonia (Mori and Sugimoto, 2015; Mori et al., 2008). In all of these pathologic conditions, the correlation between *Pneumocystis* colonization or infection and iBALT formation is unknown. However, future studies examining the relationship between *Pneumocystis* and iBALT formation in humans would be highly informative in supporting and/or validating the findings in a murine model of *Pneumocystis* exposure.

EXPERIMENTAL PROCEDURES

Mice

All mouse colonies were maintained in the Rangos Research Building Animal Facility and use was approved and performed in accordance with the University of Pittsburgh Institutional Care and Use Committee (Protocol: 14084329 and 16027674). C57BL/6, BALB/c, *Cxcr5*$^{-/-}$, *Lta*$^{-/-}$, *Stat6*$^{-/-}$, *Gata1*^{tm6Sho}/J, *Rag1*$^{-/-}$, and *Rag2*$^{-/-}$*Il2rg*$^{-/-}$ mice were all ordered from The Jackson Laboratory. The *Il17ra*$^{-/-}$ and *Il17rb*$^{-/-}$ mice were generated at Amgen. The *Il17rc*$^{-/-}$ mice were generated at GenenTech. Both male and female mice were used throughout experiments in an equal manner. Mice ranged from 6-8 weeks old, unless otherwise specified. Mice were randomized based on cage. Sample size was determined using power calculations based on prior experiments at day 14 post-infection that showed a 6-fold reduction in *Pneumocystis* burden with a 10% SD. With a type I error rate of 0.05 and a power of 0.90, we calculated the use of at least four mice per group.

Reagents

Mice were depleted of CD4^{+} cells by weekly intraperitoneal injection of 0.3 mg of GK1.5 monoclonal antibody as previously described (Eddens et al., 2015, 2016). CD20^{+} cells were depleted using intraperitoneal injections of 0.1 mg 5D2 monoclonal antibody every 3 days (Elsegeiny et al., 2015). Recombinant IL-17A and IL-13 (R&D Systems) was used at a final concentration of

100 ng/mL. Recombinant IL-6 (R&D Systems) was used at a final concentration of 40 ng/mL.

Pneumocystis Inoculation

Pneumocystis murina was harvested from the lungs of an infected *Rag2*$^{-/-}$*Il2rg*$^{-/-}$ mouse. Following straining through a 70-μm sterile filter, mice were challenged with 2.0 × 10^6 cysts/mL as previously described (Zheng et al., 2001, 2005). *Aspergillus fumigatus* inoculation was performed as described previously (McAleer et al., 2016).

Immunofluorescence Staining and Histologic Analysis

The left lobe was fixed by injecting 10% formalin into the left main stem bronchus. Lung tissue was processed, paraffin-embedded, and sectioned. H&E staining was performed by the Children's Hospital of Pittsburgh Histology Core. For immunofluorescence, slides were hydrated in PBS and were blocked for 30 min at room temperature in Fc block (10 μg/mL) and 5% v/v normal donkey serum in PBS. Slides were then incubated with primary antibodies diluted in 0.1% Tween 20 and 0.1% Triton X-100 dissolved in PBS for 30 min at room temperature to detect high endothelial venules (PNAd, clone MECA-79, BD Biosciences), lymphatics (Lyve-1, Acris, DP3513), and B cell follicles (APC-CD45R/B220, clone RA3-6B2, BD Biosciences). Germinal center B cells were visualized with a combination of proliferating cell nuclear antigen (PCNA, clone C-20, Santa Cruz Biotechnology), FITC-conjugated peanut agglutinin (PNA, L-7381-5MG, SIGMA), and APC conjugates rat anti-mouse CD45R/B220 (clone RA3-6B2, BD Biosciences). Antibodies specific for CD3-epsilon (clone M-20, Santa Cruz Biotechnology) in combination with APC-CD45R/B220 were used to define B and T cell distribution in iBALT structures. Slides were stained with a combination of antibodies specific for CD21-CD35 (clone7E9, Biolegend) and FDCM1 (551320, BD PharMingen) to detect follicular dendritic cells. Location of CXCL13-producing cells was performed with a goat anti-mouse antibody against CXCL13 (AF470, R&D Systems). To detect primary antibodies, we used Cy3-goat anti-rat Ig M (112-166-075, Jackson Immunoresearch Laboratories), Alexa Fluor 488 donkey anti-rabbit Ig G (711-546-152, Jackson Immunoresearch Laboratories), Alexa Fluor 568 donkey anti-goat Ig G (A11057, Life Technologies), Alexa Fluor 488 rabbit anti-fluorescein (A11090, Life Technologies), Alexa Fluor donkey anti-rat Ig G (A21208, Life Technologies), and Alexa Fluor 488 streptavidin (S11223, Life Technologies). After staining, tissues were mounted with prolong gold antifade with DAPI (P36931, Life Technologies). Images were collected with Zeiss Axioplan 2 microscope and the outline tool in Zeiss Axiovision software was used for measuring and enumerating lymphoid follicles in *Pneumocystis* infected lungs. Immunofluorescent staining and quantification was performed in a blinded manner.

qRT-PCR

The right middle lobe was homogenized in Trizol (Life Technologies) followed by RNA isolation per manufacturer's instructions. Following quantification using a Nanodrop 2000 (Thermo Scientific), 500 ng of RNA was converted to cDNA using iScript (Bio-Rad). Gene expression analyses were then performed using SsoAdvanced qRT-PCR universal probes supermix (Bio-Rad). Murine primers included: *Ccl19*, *Ccl21*, *Ifng*, *Prg2*, *Il6*, *Il17a*, and *Ccl11* (Applied Biosciences) and *Cxcl13*, *Il5*, *Il13*, and *Cxcl1* (IDT). *Pneumocystis* SSU burden was quantified as described previously (Eddens et al., 2016). *Hprt* was used as the housekeeping gene for calculation of relative expression and fold change.

Adoptive Transfer of CD4$^+$ T Cells

Spleens, mediastinal lymph nodes (mLN), and lungs were isolated from C57BL/6 mice infected with *Pneumocystis* for 14 days. The organs were mechanically digested and strained through a 70-μm filter and CD4$^+$ cells were isolated using an EasySep Negative selection kit (StemCell) as previously described (Elsegeiny et al., 2015). The cells were then enumerated and 5.0 × 10^5 cells were transferred intravenously to *Rag1*$^{-/-}$ mice previously infected with *Pneumocystis* for 14 days. Fourteen days following transfer, burden and gene expression was analyzed.

Ex Vivo Antigen Restimulation Assay

The right lower lobe of lung was collected, mechanically digested, and enzymatically digested with collagenase/DNase for 1 hr at 37°C as described previously (Eddens et al., 2015, 2016). Single cell suspensions were then strained using a 70-μm sterile filter. Red blood cells were lysed using a NH_4Cl solution and the cells were enumerated using Trypan Blue staining. Cells were then plated at 5 × 10^5 cells per well, stimulated with either 5 μg *Pneumocystis* antigen or 2.5 μL of CD3/CD28 Dynabeads (2015-07, Life Technologies). Following 72 hr, the cells were pelleted and the supernatants were collected and analyzed on a 7-plex T cell Luminex per manufacturer's instructions (Bio-Rad). The remaining cells were resuspended in Trizol LS (Life Technologies) for RNA isolation.

Anti-pneumocystis IgG ELISA

Serum was isolated from mice at the time of sacrifice, diluted 1:64, and used in a direct ELISA as described previously (Eddens et al., 2016).

Flow Cytometry

Whole lung cells were isolated prepared as described in the ex vivo whole lung cell stimulation methods. Briefly, cells were plated, centrifuged, and stimulated with 50 ng/mL PMA and 750 ng/mL ionomycin for 4 hr. After 1 hr, 1 μL GolgiStop (BD PharMingen) was added. Following incubation, cells were then washed and resuspended in surface antibodies diluted in PBS at 1:200 unless otherwise specified. Surface staining included: CD3-Alexa700 (eBioscience, clone: 17A2) TCRβ-PerCP-Cy5.5 (eBioscience, clone: H57-597), TCRγδ-FITC (eBioscience, clone: GL3), CD90.2-PE-Cy7, diluted 1:1,500 (eBioscience, clone: 53-2.1), CD11b-Biotin (eBioscience, clone: M1/70), F4/80-biotin (eBioscience, clone: BM8), NK1.1-biotin (BD PharMingen, clone: PK136), CD11c-biotin (BD PharMingen, clone: HL3), CD19-biotin (BD PharMingen, clone: 1D3), and TER119-biotin (BD PharMingen, cat: 553672). Following a 1 hr incubation at 4°C, cells were washed and resuspended in the streptavidin-BV421 (diluted 1:200). Following a 30 min incubation at 4°C, cells were washed and fixed and permeabilized using the eBioscience FoxP3 staining kit per manufacturer's instructions. Intracellular antibodies, anti-IL-17A-APC (eBioscience, clone: 17B7) and anti-IL-13-PE (eBioscience, clone: eBio13A) antibodies were added and incubated at 4°C for 1 hr. Cells were then washed, resuspended, and analyzed on a BD LSR II Flow Cytometer with compensation via OneComp eBeads (eBioscience). Data analysis was conducted using FlowJo software (Treestar). For sorting of pulmonary cell populations, the following antibodies were used: anti-CD45 (eBioscience, FITC 11-0454-81 and e450 48-0454-80, clone: 104) anti-CD31 (APC, eBioscience 17-0311-80 clone: 360), and anti-podoplanin (PE, eBioscience 12-5381-80 clone: 8.1.1). Cells were sorted using FacsAriaII flow cytometer into Trizol and RNA was isolated as above.

Pulmonary Fibroblast Culture and Stimulation

Whole lung cells were isolated as described above and plated at a 1:10 dilution in 24-well plates. Cells were incubated for 3 days at 37°C to allow for adherence, washed once with PBS, and left to grow in complete IMDM until reaching 50%–70% confluence. The cells were then stimulated with the various cytokine mixtures described above and incubated at 37°C for 6 or 24 hr. For adenovirus-Cre GFP (Ad-Cre) experiments, 1 μL of 2.0 × 10^{12} plaque-forming units (pfu) of Ad-Cre was added at the point of 100% confluence and incubated at 37°C for 48 hr. Cells were then washed and stimulated as described above. The cells were then harvested in 1 mL Trizol to isolate total RNA and perform qRT-PCR.

Statistics

Each data point represents a biologic replicate. Every experiment was performed twice at minimum. All statistical analyses were performed using GraphPad Prism version 6.0f. All data are presented as mean ± SEM. Each group was analyzed for outliers using the ROUT method with a Q = 1%. Studies with two groups were analyzed with a Student's t test. Studies with three or more groups were analyzed using an ordinary one-way ANOVA with Tukey's multiple comparisons. Differences with a $p < 0.05$ were considered statistically significant.

SUPPLEMENTAL INFORMATION

Supplemental Information includes Supplemental Experimental Procedures and seven figures and can be found with this article online at http://dx.doi.org/10.1016/j.celrep.2017.03.016.

AUTHOR CONTRIBUTIONS

Conceptualization: T.E., K.C., and J.K.K; Methodology: T.E., K.C., and J.K.K.; Validation: T.E.; Formal Analysis: T.E.; Investigation: T.E., W.E., J.R.-M., P.C., K.S., M.L.G.-H., G.T.-N., B.T.C., and K.C.; Resources: J.R.M., S.A.K., and J.K.K.; Writing – Original Draft: T.E., and J.R.M.; Writing – Review & Editing: T.E., J.R.-M., P.C., K.S., W.E., M.L.G.H., B.T.C., S.A.K., K.C., and J.K.K.; Visualization: T.E. and J.R.-M.; Funding Acquisition: J.K.K.

ACKNOWLEDGMENTS

This work was supported by grants from the NIH (F30AI114146 to T.E., R01HL062052 and R01AI20033 to J.K.K., and K08HL128809 to B.C.). J.R.-M. is supported by the Department of Medicine at the University of Rochester (NIAID grant RO1AI111914). The anti-CD20 antibody (5D2) was generously provided by Andrew Chan, Genentech. The Gata3$^{fl/fl}$ mice were a gift from the late William Paul, NIH.

Received: June 16, 2016
Revised: February 2, 2017
Accepted: March 2, 2017
Published: March 28, 2017

REFERENCES

Bracke, K.R., Verhamme, F.M., Seys, L.J., Bantsimba-Malanda, C., Cunoosamy, D.M., Herbst, R., Hammad, H., Lambrecht, B.N., Joos, G.F., and Brusselle, G.G. (2013). Role of CXCL13 in cigarette smoke-induced lymphoid follicle formation and chronic obstructive pulmonary disease. Am. J. Respir. Crit. Care Med. *188*, 343–355.

Cyster, J.G. (2003). Lymphoid organ development and cell migration. Immunol. Rev. *195*, 5–14.

De Togni, P., Goellner, J., Ruddle, N.H., Streeter, P.R., Fick, A., Mariathasan, S., Smith, S.C., Carlson, R., Shornick, L.P., Strauss-Schoenberger, J., et al. (1994). Abnormal development of peripheral lymphoid organs in mice deficient in lymphotoxin. Science *264*, 703–707.

Demoor, T., Bracke, K.R., Maes, T., Vandooren, B., Elewaut, D., Pilette, C., Joos, G.F., and Brusselle, G.G. (2009). Role of lymphotoxin-alpha in cigarette smoke-induced inflammation and lymphoid neogenesis. Eur. Respir. J. *34*, 405–416.

Eddens, T., and Kolls, J.K. (2015). Pathological and protective immunity to Pneumocystis infection. Semin. Immunopathol. *37*, 153–162.

Eddens, T., Elsegeiny, W., Nelson, M.P., Horne, W., Campfield, B.T., Steele, C., and Kolls, J.K. (2015). Eosinophils Contribute to Early Clearance of Pneumocystis murina Infection. J. Immunol. *195*, 185–193.

Eddens, T., Campfield, B.T., Serody, K., Manni, M.L., Horne, W., Elsegeiny, W., McHugh, K.J., Pociask, D., Chen, K., Zheng, M., et al. (2016). A novel CD4(+) T cell-dependent murine model of Pneumocystis-driven asthma-like pathology. Am. J. Respir. Crit. Care Med. *194*, 807–820.

Elliot, J.G., Jensen, C.M., Mutavdzic, S., Lamb, J.P., Carroll, N.G., and James, A.L. (2004). Aggregations of lymphoid cells in the airways of nonsmokers, smokers, and subjects with asthma. Am. J. Respir. Crit. Care Med. *169*, 712–718.

Elsegeiny, W., Eddens, T., Chen, K., and Kolls, J.K. (2015). Anti-CD20 antibody therapy and susceptibility to Pneumocystis pneumonia. Infect. Immun. *83*, 2043–2052.

Emery, J.L., and Dinsdale, F. (1973). The postnatal development of lymphoreticular aggregates and lymph nodes in infants' lungs. J. Clin. Pathol. *26*, 539–545.

Fitzpatrick, M.E., Tedrow, J.R., Hillenbrand, M.E., Lucht, L., Richards, T., Norris, K.A., Zhang, Y., Sciurba, F.C., Kaminski, N., and Morris, A. (2014). Pneumocystis jirovecii colonization is associated with enhanced Th1 inflammatory gene expression in lungs of humans with chronic obstructive pulmonary disease. Microbiol. Immunol. *58*, 202–211.

Fleige, H., Ravens, S., Moschovakis, G.L., Bölter, J., Willenzon, S., Sutter, G., Häussler, S., Kalinke, U., Prinz, I., and Förster, R. (2014). IL-17-induced CXCL12 recruits B cells and induces follicle formation in BALT in the absence of differentiated FDCs. J. Exp. Med. *211*, 643–651.

Fletcher, A.L., Malhotra, D., Acton, S.E., Lukacs-Kornek, V., Bellemare-Pelletier, A., Curry, M., Armant, M., and Turley, S.J. (2011). Reproducible isolation of lymph node stromal cells reveals site-dependent differences in fibroblastic reticular cells. Front. Immunol. *2*, 35.

Foo, S.Y., and Phipps, S. (2010). Regulation of inducible BALT formation and contribution to immunity and pathology. Mucosal Immunol. *3*, 537–544.

Gaffen, S.L. (2009). Structure and signalling in the IL-17 receptor family. Nat. Rev. Immunol. *9*, 556–567.

GeurtsvanKessel, C.H., Willart, M.A., Bergen, I.M., van Rijt, L.S., Muskens, F., Elewaut, D., Osterhaus, A.D., Hendriks, R., Rimmelzwaan, G.F., and Lambrecht, B.N. (2009). Dendritic cells are crucial for maintenance of tertiary lymphoid structures in the lung of influenza virus-infected mice. J. Exp. Med. *206*, 2339–2349.

Gopal, R., Rangel-Moreno, J., Slight, S., Lin, Y., Nawar, H.F., Fallert Junecko, B.A., Reinhart, T.A., Kolls, J., Randall, T.D., Connell, T.D., and Khader, S.A. (2013). Interleukin-17-dependent CXCL13 mediates mucosal vaccine-induced immunity against tuberculosis. Mucosal Immunol. *6*, 972–984.

Goya, S., Matsuoka, H., Mori, M., Morishita, H., Kida, H., Kobashi, Y., Kato, T., Taguchi, Y., Osaki, T., Tachibana, I., et al. (2003). Sustained interleukin-6 signalling leads to the development of lymphoid organ-like structures in the lung. J. Pathol. *200*, 82–87.

Halle, S., Dujardin, H.C., Bakocevic, N., Fleige, H., Danzer, H., Willenzon, S., Suezer, Y., Hämmerling, G., Garbi, N., Sutter, G., et al. (2009). Induced bronchus-associated lymphoid tissue serves as a general priming site for T cells and is maintained by dendritic cells. J. Exp. Med. *206*, 2593–2601.

John-Schuster, G., Hager, K., Conlon, T.M., Irmler, M., Beckers, J., Eickelberg, O., and Yildirim, A.Ö. (2014). Cigarette smoke-induced iBALT mediates macrophage activation in a B cell-dependent manner in COPD. Am. J. Physiol. Lung Cell. Mol. Physiol. *307*, L692–L706.

Kocks, J.R., Davalos-Misslitz, A.C., Hintzen, G., Ohl, L., and Förster, R. (2007). Regulatory T cells interfere with the development of bronchus-associated lymphoid tissue. J. Exp. Med. *204*, 723–734.

Lee, J.J., McGarry, M.P., Farmer, S.C., Denzler, K.L., Larson, K.A., Carrigan, P.E., Brenneise, I.E., Horton, M.A., Haczku, A., Gelfand, E.W., et al. (1997). Interleukin-5 expression in the lung epithelium of transgenic mice leads to pulmonary changes pathognomonic of asthma. J. Exp. Med. *185*, 2143–2156.

Litsiou, E., Semitekolou, M., Galani, I.E., Morianos, I., Tsoutsa, A., Kara, P., Rontogianni, D., Bellenis, I., Konstantinou, M., Potaris, K., et al. (2013). CXCL13 production in B cells via Toll-like receptor/lymphotoxin receptor signaling is involved in lymphoid neogenesis in chronic obstructive pulmonary disease. Am. J. Respir. Crit. Care Med. *187*, 1194–1202.

Maini, R., Henderson, K.L., Sheridan, E.A., Lamagni, T., Nichols, G., Delpech, V., and Phin, N. (2013). Increasing Pneumocystis pneumonia, England, UK, 2000-2010. Emerg. Infect. Dis. *19*, 386–392.

McAleer, J.P., Nguyen, N.L., Chen, K., Kumar, P., Ricks, D.M., Binnie, M., Armentrout, R.A., Pociask, D.A., Hein, A., Yu, A., et al. (2016). Pulmonary th17 antifungal immunity is regulated by the gut microbiome. J. Immunol. *197*, 97–107.

Mikaelsson, L., Jacobsson, G., and Andersson, R. (2006). Pneumocystis pneumonia–a retrospective study 1991-2001 in Gothenburg, Sweden. J. Infect. *53*, 260–265.

Mori, S., and Sugimoto, M. (2015). Pneumocystis jirovecii Pneumonia in Rheumatoid Arthritis Patients: Risks and Prophylaxis Recommendations. Clin. Med. Insights Circ. Respir. Pulm. Med. *9* (*Suppl 1*), 29–40.

Mori, S., Cho, I., Ichiyasu, H., and Sugimoto, M. (2008). Asymptomatic carriage of Pneumocystis jiroveci in elderly patients with rheumatoid arthritis in Japan: a possible association between colonization and development of Pneumocystis jiroveci pneumonia during low-dose MTX therapy. Mod. Rheumatol. *18*, 240–246.

Morris, A., Lundgren, J.D., Masur, H., Walzer, P.D., Hanson, D.L., Frederick, T., Huang, L., Beard, C.B., and Kaplan, J.E. (2004a). Current epidemiology of Pneumocystis pneumonia. Emerg. Infect. Dis. *10*, 1713–1720.

Morris, A., Sciurba, F.C., Lebedeva, I.P., Githaiga, A., Elliott, W.M., Hogg, J.C., Huang, L., and Norris, K.A. (2004b). Association of chronic obstructive pulmonary disease severity and Pneumocystis colonization. Am. J. Respir. Crit. Care Med. *170*, 408–413.

Moyron-Quiroz, J.E., Rangel-Moreno, J., Kusser, K., Hartson, L., Sprague, F., Goodrich, S., Woodland, D.L., Lund, F.E., and Randall, T.D. (2004). Role of inducible bronchus associated lymphoid tissue (iBALT) in respiratory immunity. Nat. Med. *10*, 927–934.

Moyron-Quiroz, J.E., Rangel-Moreno, J., Hartson, L., Kusser, K., Tighe, M.P., Klonowski, K.D., Lefrançois, L., Cauley, L.S., Harmsen, A.G., Lund, F.E., and Randall, T.D. (2006). Persistence and responsiveness of immunologic memory in the absence of secondary lymphoid organs. Immunity *25*, 643–654.

Norris, K.A., and Morris, A. (2011). Pneumocystis infection and the pathogenesis of chronic obstructive pulmonary disease. Immunol. Res. *50*, 175–180.

Pérez, F.J., Ponce, C.A., Rojas, D.A., Iturra, P.A., Bustamante, R.I., Gallo, M., Hananias, K., and Vargas, S.L. (2014). Fungal colonization with Pneumocystis correlates to increasing chloride channel accessory 1 (hCLCA1) suggesting a pathway for up-regulation of airway mucus responses, in infant lungs. Results Immunol. *4*, 58–61.

Pitzalis, C., Jones, G.W., Bombardieri, M., and Jones, S.A. (2014). Ectopic lymphoid-like structures in infection, cancer and autoimmunity. Nat. Rev. Immunol. *14*, 447–462.

Randall, T.D. (2010). Pulmonary dendritic cells: thinking globally, acting locally. J. Exp. Med. *207*, 451–454.

Rangel-Moreno, J., Hartson, L., Navarro, C., Gaxiola, M., Selman, M., and Randall, T.D. (2006). Inducible bronchus-associated lymphoid tissue (iBALT) in patients with pulmonary complications of rheumatoid arthritis. J. Clin. Invest. *116*, 3183–3194.

Rangel-Moreno, J., Moyron-Quiroz, J.E., Hartson, L., Kusser, K., and Randall, T.D. (2007). Pulmonary expression of CXC chemokine ligand 13, CC chemokine ligand 19, and CC chemokine ligand 21 is essential for local immunity to influenza. Proc. Natl. Acad. Sci. USA *104*, 10577–10582.

Rangel-Moreno, J., Carragher, D.M., de la Luz Garcia-Hernandez, M., Hwang, J.Y., Kusser, K., Hartson, L., Kolls, J.K., Khader, S.A., and Randall, T.D. (2011). The development of inducible bronchus-associated lymphoid tissue depends on IL-17. Nat. Immunol. *12*, 639–646.

Respaldiza, N., Medrano, F.J., Medrano, A.C., Varela, J.M., de la Horra, C., Montes-Cano, M., Ferrer, S., Wichmann, I., Gargallo-Viola, D., and Calderon, E.J. (2004). High seroprevalence of Pneumocystis infection in Spanish children. Clin. Microbiol. Infect. *10*, 1029–1031.

Rickel, E.A., Siegel, L.A., Yoon, B.R., Rottman, J.B., Kugler, D.G., Swart, D.A., Anders, P.M., Tocker, J.E., Comeau, M.R., and Budelsky, A.L. (2008). Identification of functional roles for both IL-17RB and IL-17RA in mediating IL-25-induced activities. J. Immunol. *181*, 4299–4310.

Tschernig, T., Kleemann, W.J., and Pabst, R. (1995). Bronchus-associated lymphoid tissue (BALT) in the lungs of children who had died from sudden infant death syndrome and other causes. Thorax *50*, 658–660.

Vargas, S.L., Ponce, C.A., Gallo, M., Pérez, F., Astorga, J.F., Bustamante, R., Chabé, M., Durand-Joly, I., Iturra, P., Miller, R.F., et al. (2013). Near-universal prevalence of Pneumocystis and associated increase in mucus in the lungs of infants with sudden unexpected death. Clin. Infect. Dis. *56*, 171–179.

Zheng, M., Shellito, J.E., Marrero, L., Zhong, Q., Julian, S., Ye, P., Wallace, V., Schwarzenberger, P., and Kolls, J.K. (2001). CD4+ T cell-independent vaccination against Pneumocystis carinii in mice. J. Clin. Invest. *108*, 1469–1474.

Zheng, M., Ramsay, A.J., Robichaux, M.B., Kliment, C., Crowe, C., Rapaka, R.R., Steele, C., McAllister, F., Shellito, J.E., Marrero, L., et al. (2005). CD4+ T cell-independent DNA vaccination against opportunistic infections. J. Clin. Invest. *115*, 3536–3544.